Draft version September 3, 2011
Preprint typeset using LaTeX style emulateapj v. 11/10/09

# ELEMENT ABUNDANCE OF GAS AROUND $\beta$ PICTORIS

Ji-Wei Xie[1,3], Alexis Brandeker[2], Yanqin Wu[1]
[1]Department of Astronomy and Astrophysics, University of Toronto, Toronto, ON M5S 3H4, Canada;
[2]Department of Astronomy, Stockholm University, SE-106 91 Stockholm, Sweden and
[3]Department of Astronomy & Key Laboratory of Modern Astronomy and Astrophysics in Ministry of Education, Nanjing University, 210093, China

*Draft version September 3, 2011*

## ABSTRACT

Recent observations have shown that carbon in the gas around $\beta$ Pictoris is $> 100$ times overabundant with respect to the solar abundance. Although it is thought that such an overabundant in carbon is crucial to retain the metal elements in the disk, its origin is however unclear. In this paper, we establish a simple analytical model to study gas removing process and thus calculate the abundance of various elements in the gas disk around $\beta$ Pictoris. Gas removing rate is controlled by the inward flow-viscosity accretion-and the outward flow-radiation drift. If the disk viscosity (using classical $\alpha$ disk model) is low, thus radiation drift dominates the gas loss, then carbon can become highly overabundant. In order to produce the observed overabundance of carbon, a low viscosity of $\alpha < 10^{-3}$ and a gas production with solar abundance are preferred.

## 1. INTRODUCTION

A debris disk is a circumstellar disk of dust and debris in orbit around a star. The dust in debris disk is generally considered being produced by cascade collisions which grind down large particles (planetesimals) to the observed small grains (Wyatt 2008; Krivov 2010). Although most detected debris disks are lacking of gas, people did find significant gas in the debris disk around $\beta$ Pictoris (Hobbs et al. 1985), which is the subject of this work.

Some metallic gas components, such as neutral sodium (Na I), are found to be in stable orbits with small radial velocities (Olofsson et al. 2001; Brandeker et al. 2004). This was not expected as Na I should be subject to very strong radiation pressure (the ratio of radiation force and gravitational force being $\beta \sim 360$). For such a reason, some agent is needed to brake these metallic gas down to low observed radial velocity. As suggested by Fernández et al. (2006), if the gas is overabundant in carbon by a factor $\geq 10$, then then the gas can be self-braking. Indeed, such a carbon rich gas has already been discovered (Roberge et al. 2006), and it could be produced through collisional vaporization of the dust (Czechowski & Mann 2007) or by photo desorption (Chen et al. 2007).

Furthermore, the latest observations (Brandeker et al. 2011) shows that the C and O are $\sim 400$ times overabundant relative to cosmic (solar) abundance (in solar abundance, ratio of C and Fe density is $\sim 10$) . Such a large overabundant in C and O cannot be reproduced directly by collisional vaporization of the dust. Instead, it might indicate that the gas disk has underwent some certain evolution processes which increase the abundances of C and O to current high values. One possibility is that various elements experience various radiation pressure, and thus are removed at different rates. Since C and O do not experience any significant radiation pressure, they would stay behind and thus become enhanced relative to other elements.

xiejiwei@gmail.com

In this work, we are going to study such a process for various elements with a simple analytical model, focusing on the relative abundance evolution of various elements. This paper is organized as the following. We describe our analytical model in section 2, with some related derivations in detail can be found in the Appendix A and B. Our results and comparison to observations are discussed in section 3. Finally, we conclude in section 4.

## 2. MODEL

### 2.1. *Collision VS. Radiation Drift*

A particle (ion or neutral atom) with $\beta > 0.5$ is accelerated to drift outward due to the radiation force, and at the same time it is decelerated through collisions with other braking particles that are not subjected to significant radiation force. The dominant braking particles are carbon ions (C II). The competing process between radiation acceleration and collision deceleration leads to an equilibrium drift velocity.

For a neutral tracer particle, its equilibrium drift velocity is (see the Appendix A for detailed derivation)

$$v_{\mathrm{neu\_1}} \sim 0.8\beta\left(\frac{m_x}{m_c}\right)\left(\frac{m_x m_c}{m_p(m_x+m_c)}\right)^{1/2}\left(\frac{N_{C_{II}}}{100\,\mathrm{cm}^{-3}}\right)^{-1} \left(\frac{r}{100\,\mathrm{AU}}\right)^{-2}\left(\frac{M_{star}}{\mathrm{M}_\odot}\right)\left(\frac{Pol}{10\,\mathrm{\AA}^3}\right)^{-1/2}\ \mathrm{ms}^{-1}, \quad (1)$$

where $m_p$, $m_x$ are the mass of a proton and a atom of element "x", respectively, r is the radial distance to the center star of mass $M_{star}$, $N_{C_{II}}$ is the number density of $C_{II}$, and $Pol$ is the polarizability of neutral atom "x". On the other hand, there is another limiting velocity ($v_{\mathrm{neu\_2}}$) that the particle can reach before it is ionized,

$$v_{\mathrm{neu\_2}} \sim \beta\frac{GM_{star}}{r^2}\frac{1}{\Gamma} \sim 10(\beta-0.5)\left(\frac{\Gamma_{AU}}{10^{-7}\,\mathrm{s}^{-1}}\right)\ \mathrm{ms}^{-1}, \quad (2)$$

where $G$ is the gravity constant, $\Gamma_{AU}$ is the ionization rate, $\Gamma$, of the neutral atom "x" at $r = 1$ AU. Following Brandeker (2011) [1], the expected velocity of the neutral tracer is

$$v_{\rm neu} = \frac{\gamma\, v_{\rm neu\_2}}{\gamma + 1} \quad (3)$$

, where $\gamma = v_{\rm neu\_1}/v_{\rm neu\_2}$.

For an ionized tracer particle, its equilibrium drift velocity due to collisions with carbon ions can be derived as (see the appendix B for detailed derivation)

$$v_{\rm ion} \sim 3.7\times10^{-2}\beta\left[\frac{m_x^2}{m_c(m_c+m_x)}\right]^{1/2}\left(\frac{N_{C_{II}}}{100\,{\rm cm}^{-3}}\right)^{-1/2} \left(\frac{r}{100\,{\rm AU}}\right)^{-1}\left(\frac{M_{star}}{{\rm M}_\odot}\right)^{1/2}\left(\frac{T_{disk}}{100\,{\rm K}}\right)\ {\rm ms}^{-1} \quad (4)$$

Therefore, the total effective drift velocity of tracer "x", which is driven by radiation force, is

$$u_x = f_x v_{\rm neu} + (1 - f_x) v_{\rm ion}, \quad (5)$$

where $f_x$ is the neutral fraction of element "x", which can be calculated from the equation of ionization equilibrium (see Appendix C).

Figure 1 shows $v_{\rm neu\_1}, v_{\rm neu\_2}, v_{\rm neu}$ and $v_{\rm ion}$ for all the elements with $\beta > 0.5$.

- (1) From the top panel of figure 1, we see that most elements' neutral drift velocities $v_{\rm neu}$ are close to $v_{\rm neu\_2}$ (ionization limit), except for Be, B, Na, Mg, P, S, and Co for which $v_{\rm neu\_2}$ (neutral-ion collision limit) begins to affect $v_{\rm neu}$.
- (2) Form the bottom panel of figure 1, we see that neutral dirft ($v_{\rm neu} * f_x$ dominates the final effective outward drift for most elements, except for Ca.

### 2.2. *Viscosity Accretion VS. Radiation Drift*

Beside the outward drift driven by radiation, gas particles are also subject to viscosity accretion toward the central star. The typical timescale for viscosity accretion ($t_v$) and for radiation drift ($t_r$) can be estimated as the follows

$$t_v \sim \frac{r^2}{\nu} \sim 1.4\times10^5\left(\frac{\alpha}{0.1}\right)^{-1}\left(\frac{r}{100\,{\rm AU}}\right)\ {\rm yr} \quad (6)$$

$$t_r \sim \frac{r}{u_x} \sim 4.7\times10^5\left(\frac{u_x}{1\,{\rm m\,s}^{-1}}\right)^{-1}\left(\frac{r}{100\,{\rm AU}}\right)\ {\rm yr}. \quad (7)$$

Equating $t_v$ and $t_r$, then the critical $\alpha$, at which the inflow driven by viscosity accretion is comparable to the outflow driven by radiation force, can be derived as

$$\alpha_{cr} \sim 0.33\left(\frac{u_x}{1\,{\rm m\,s}^{-1}}\right). \quad (8)$$

[1] Note that the different names of some variables as compared to those in Brandeker (2011). The two neutral limiting velocities, $v_{neu\_1}$ and $v_{neu\_2}$, are corresponding to the $v_{drift}$ and $v_{ion}$ in Brandeker (2011), while $v_{ion}$ in this paper denotes the limiting velocity of ionized tracer particles.

### 2.3. *Abundance Ratio:* $\left[\frac{N_c}{N_x}\right]$

#### 2.3.1. *equilibrium case*

Once the equilibrium is realized, gas production rate should be equating to the gas removing rate. For those elements that are subject to little radiation force, such as carbon, their removing rates are only governed by the viscosity accretion inflow, while for elements that are subject to significant radiation force, such as sodium, their removing rates are governed by both the viscosity accretion inflow and the radiation drift outflow. Hence, the equilibrium equations (zero-order estimate [2] ) for the field gas particle, carbon, and for the tracer particle, "x", can be written as

$$-\frac{\Sigma_c}{t_v} + S_c \sim 0 \quad (9)$$

$$-\frac{\Sigma_x}{t_r} - \frac{\Sigma_x}{t_v} + S_x \sim 0 \quad (10)$$

where $S_c$ and $S_x$ denote the gas production rate of carbon and element "x" (see the Appendix C for details about the gas production). The equilibrium surface densities then can be solved as

$$\Sigma_c \sim S_c t_v$$
$$\Sigma_x \sim S_x\left(\frac{t_v t_r}{t_v + t_r}\right), \quad (11)$$

and the equilibrium abundance ratio between carbon and the tracer is

$$\left[\frac{N_c}{N_x}\right]_e = \frac{\Sigma_{c_e}}{\Sigma_{x_e}}\frac{m_x}{m_c} = \frac{S_c}{S_x}\frac{m_x}{m_c}\left(\frac{t_v}{t_r}+1\right), = \left[\frac{\Lambda_c}{\Lambda_x}\right]\left(\frac{t_v}{t_r}+1\right), \quad (12)$$

where $m_c$ is the atomic mass of carbon, and $\Lambda_c$, $\Lambda_x$ are the abundance of carbon and tracer "X" in the source material (see table-1 and the appendix). The time for carbon ($t_{c_e}$) and the tracer ($t_{x_e}$) to reach their equilibriums are respectively,

$$t_{c_e} = t_v,$$
$$t_{x_e} = \frac{t_v t_r}{t_v + t_r}. \quad (13)$$

As $t_{x_e} < t_{c_e}$, thus the whole system reach its equilibrium in

$$t_e = t_{c_e} = t_v, \quad (14)$$

which denpends *only* on the viscosity accretion.

#### 2.3.2. *non-equilibrium case: if* $t_{age} < t_v$

The system would not reach its equilibrium $t_{age} < t_e \equiv t_v$, where $t_{age}$ is the age of the system. Depending on the value of $t_r$, such case can be divided into two sub-cases as the following.

[2] For such an zero-order estimate, variables which depend on radial distance $r$, such as $\Sigma_c$, $\Sigma_x$, $t_r$ and $t_v$, are not treated as a distribution of $r$ but a characteristic scalar of the gas disk, namely the corresponding value at $r = R_{disk}$, where $R_{disk}$ (typically 100 AU) is the characteristic size of the gas disk.

- (1) $t_{age} > t_r$
In this sub-case, equilibrium can still be reached for the tracer at $t = t_r$ but not for the carbon, whose density will keep increasing. The maximum abundance ratio will be reached at $t_{age}$, and it can be roughly estimated as
$$\left[\frac{N_c}{N_x}\right]_{ne\_1} \sim \left[\frac{\Lambda_c}{\Lambda_x}\right]\left(\frac{t_{age}}{t_r}\right), \quad (15)$$

- (2) $t_{age} < t_r$
In this sub-case, both the time scale to remove the gas by both accretion and radiation are longer than the system age, thus gas removing can be ignored and the abundances of various elements remain as the same as when they were produced, namely
$$\left[\frac{N_c}{N_x}\right]_{ne\_2} \sim \left[\frac{\Lambda_c}{\Lambda_x}\right]. \quad (16)$$

Note, although we presuppose $\beta > 0.5$ during our derivation, our final results about the abundance ratio (Eqn.12, 15 and 16) indeed can apply to elements of any $\beta$ (just set $t_r = \infty$ for the case of $\beta \leq 0.5$).

## 3. RESULTS AND DISCUSSIONS: COMPARISON TO OBSERVATIONS

In this subsection, we compare our analytical results (Eqn.12, 15 and 16) to the observation of various elements in the gas disk around $\beta$ Pictoris (see Roberge et al. 2006).

We adopt the mass of the star $M = 1.75\mathrm{M}_\odot$, age of the system $t_{age} = 15$ Myr, typcial locaion or size of gas disk, $r = R_{\rm disk} = 100$ AU. For the viscosity coefficient ($\alpha$ in Eqn.6) we consider two cases with $\alpha = 10^{-3}$ (see figure 2) and $\alpha = 10^{-1}$ (see figure 3). In each case, we adopt two production abundance (the solar abundance and abundance of carbonaceous chondrites) as two comparing sub-cases.

As can be seen from figures 2 and 3, some major results can be summarize as the following.

- *gas production: solar v.s. carbonaceous*
Comparing the triangles between the two panels of figure 2 (also figure 3), we see the two relative production abundances (solar and carbonaceous) are roughly the same for most elements, except for H, He, C, O, N, Ne, Ar are significant more abundant for the solar. This is the reason why the two panels show nearly the same results for elements except for H, He, C, O, N, Ne, Ar. In addition, we note that many observed abundances (such as for Na, Ca, Cr, Mn, Fe, Ni) are close to their production abundances.

- *high $\alpha$ v.s. low $\alpha$*
If the viscosity is very high, such as $\alpha = 0.1$ shown in figure 3, viscosity accretion will dominate the mass loss for most elements (except for Be, P, S, Sc, and Cr which are subject to very strong radiation drift against viscosity accretion even if $\alpha = 0.1$). In such case, $t_v \ll t_r$, and thus the final element abundances are close to their production abundance according to equation 12, namely most crosses are very close to their corresponding triangles.
If the viscosity is very low, such as $\alpha = 10^{-3}$ shown in figure 2, gas loss is dominated by radiation drift. As different elements are subject to different radiation forces, they have different removing rates, thus finally changing their abundances in the system. As shown in figure 2 where elements' abundances are plot as normalized to Na, elements that subject to stronger/weaker) radiation drift than $Na$ will have their final abundances (crosses in the figure) greater/less than their production abundance (triangles in the figure).

- $N_c/N_{Na}$ and $N_c/N_{Fe}$
As suggested by the most recent observations (Brandeker 2011), carbon is thought to be over $\sim 100$ times overabundance with respect to the solar abundance if comparing to $Na$ and $Fe$. In solar abundance, gas production abundance ratio are $\Lambda c/\Lambda_{Na}$ $\sim$120, $\Lambda_c/\Lambda_{Fe} \sim 8.5$, while in carbonaceous abundance, these ratios are systematically smaller by a factor of $\sim 10$. Therefore, in order to produce the current observed abundance ratios of $N_c/N_{Na}$ and $N_c/N_{Fe}$, one needs an enhancement of $> 100$ times for $N_c/N_{Na}$ and $N_c/N_{Fe}$ if assuming a solar production abundance, $> 1000$ times if assuming a carbonaceous production abundance.
On the other hand, Na and Fe are subject to roughly the same radiation drift, with $t_r \sim 10^5$ for Na and $t_r \sim 6 \times 10^4$ yr for Fe. Thus the largest enhancement that can reach is $t_{age}/t_r$ (if $t_r \ll t_v$), namely a factor of $\sim 150$ for Na and $\sim 250$ for Fe.
Given above order of estimates, we see a low viscosity ($\alpha < 10^{-3}$) and gas production of solar abundance are preferred in order to produce the current high overabundance of carbon relative to sodium and iron.

- need better models or better data ? If we adopt $\alpha < 10^{-3}$ and a gas production of solar abundance, as can be seen in the bottom panel of figure 2, our results can fit the observed data well only for $C$ (updated by Brandeker (2011)), Na, Fe and Ni. Hence, the reason can be whether our simple model miss somethings for some elements or current observed data are not reliable for some elements. On one side, ur model is just a zero-order analysis, and the results are very sensitive to the ionization state, such as the neutral fraction, of each elements, which are computed using a very simple mode here. On the other side, the observational abundances are indeed very uncertain for some element, such as P, Mg ....

## 4. CONCLUSION

A low gas disk viscosity ($\alpha < 10^{-3}$) and a gas production of solar abundance are preferred to produce a $> 100$ times enhancement of [C/Na] or [C/Fe] (abundance ratio between carbon and sodium or iron) with respect to the solar abundance.

## 5. ACKNOWLEDGMENTS

This work was supported by the International Summer Institute for Modeling in Astrophysics (ISIMA) during the 2011 program "Star and Planet Formation" held in Kavli Institute for Astronomy and Astrophysics at Peking University. We would like to thank Pascale Garaud for valuable discussions and suggestions

REFERENCES

Beust, H., Lagrange-Henri, A. M., Vidal-Madjar, A., & Ferlet, R. 1989, A&A, 223, 304
Brandeker, A., Liseau, R., Olofsson, G., & Fridlund, M. 2004, A&A, 413, 681
Brandeker, A. 2011, ApJ, 729, 122
Chen, C. H., Li, A., Bohac, C., et al. 2007, ApJ, 666, 466
Czechowski, A., & Mann, I. 2007, ApJ, 660, 1541
Fernández, R., Brandeker, A., & Wu, Y. 2006, ApJ, 643, 509
Hobbs, L. M., Vidal-Madjar, A., Ferlet, R., Albert, C. E., & Gry, C. 1985, ApJ, 293, L29
Krivov, A. V. 2010, Research in Astronomy and Astrophysics, 10, 383
Olofsson, G., Liseau, R., & Brandeker, A. 2001, ApJ, 563, L77
Roberge, A., Feldman, P. D., Weinberger, A. J., Deleuil, M., & Bouret, J.-C. 2006, Nature, 441, 724
Wyatt, M. C. 2008, ARA&A, 46, 339

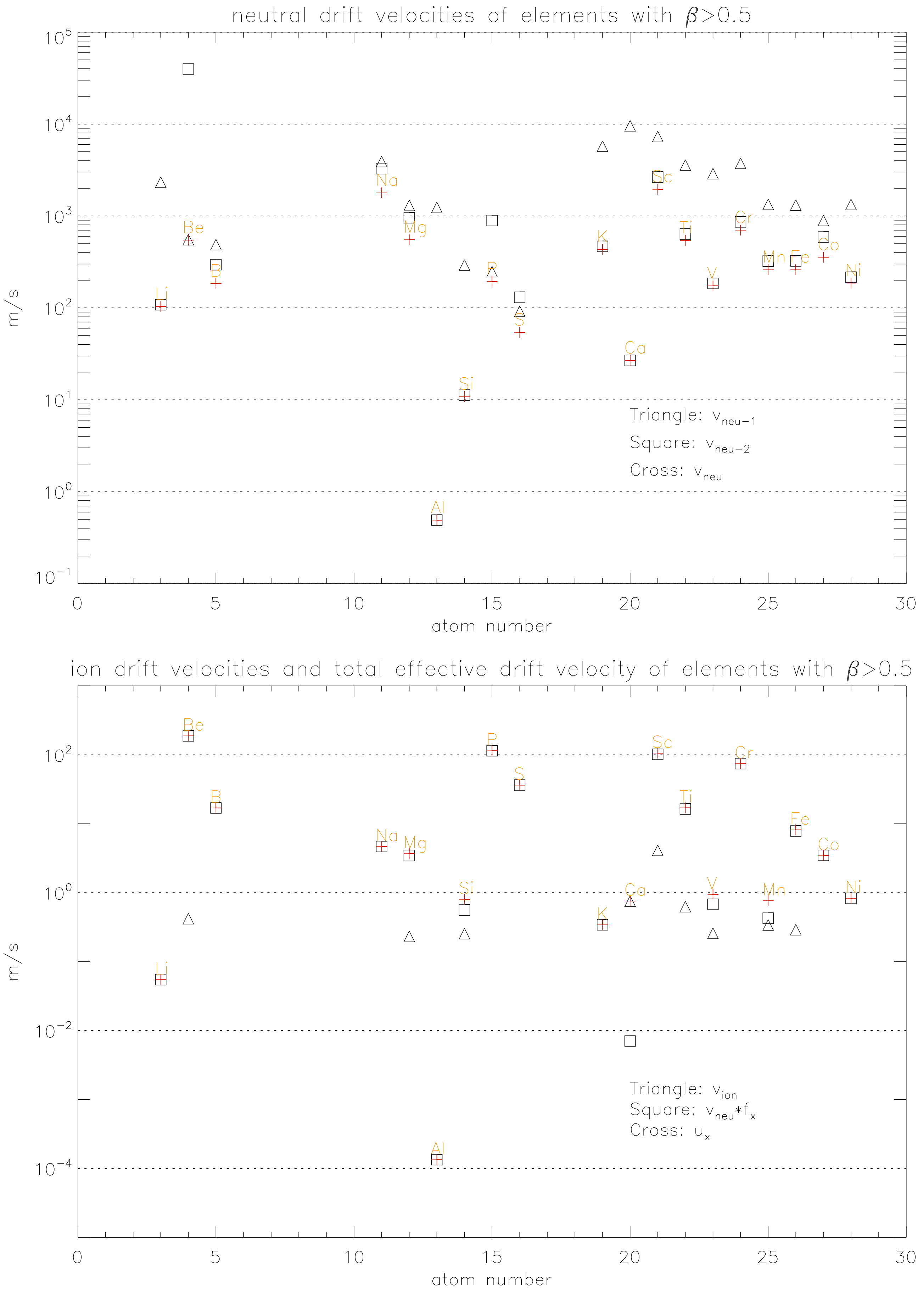


FIG. 1.— Top panel: $v_{\rm neu\_1}, v_{\rm neu\_2}$ and $v_{\rm neu}$ of elements with $\beta > 0.5$. Bottom panel: $v_{\rm ion}, f_x * v_{\rm neu}$ and $u_x$ of elements with $\beta > 0.5$. Results are calculated using equation (A7-5) with model parameters set as $N_C = 100{\rm cm}^{-3}$ (thus $N_{C_{II}}$ calculated using Eqn.C3 in the appendix C), $r = 100{\rm AU}$, $M_{star} = 1.75{\rm M}_\odot$ , $T_{disk} = 100$ k.

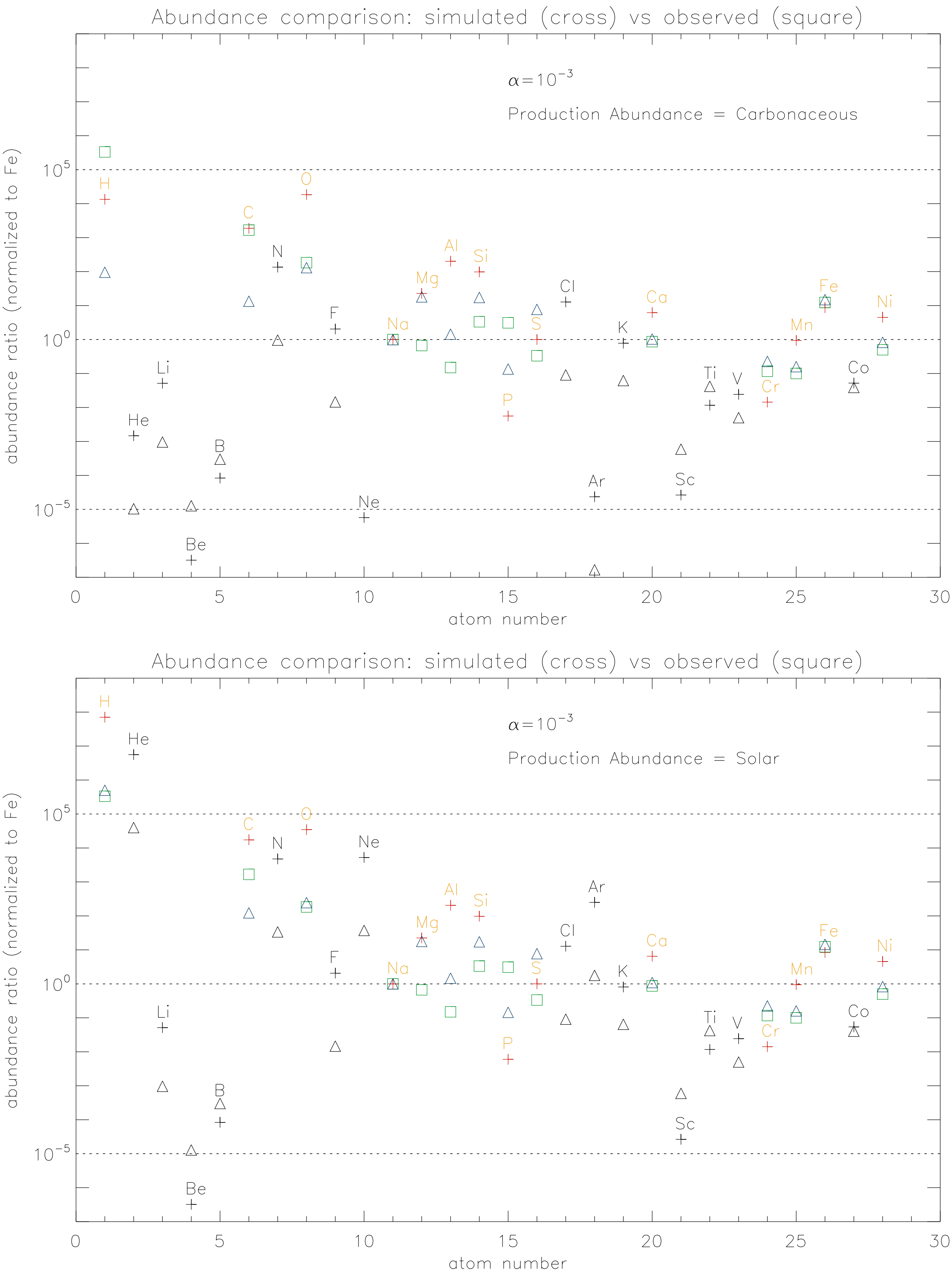


FIG. 2.— Abundance comparison to observation with $\alpha = 10^{-3}$. Production of gas is using the abundance of carbonaceous chondrites (top panel) and solar abundance (bottom). Green squares are data points from observation (Roberge et al. 2006), triangles denotes the gas production abundances, crosses are our analytical results (Eqn.12, Eqn.15 or Eqn.16). Those black crosses and triangles corresponds to the properties of elements without observed data for comparing.

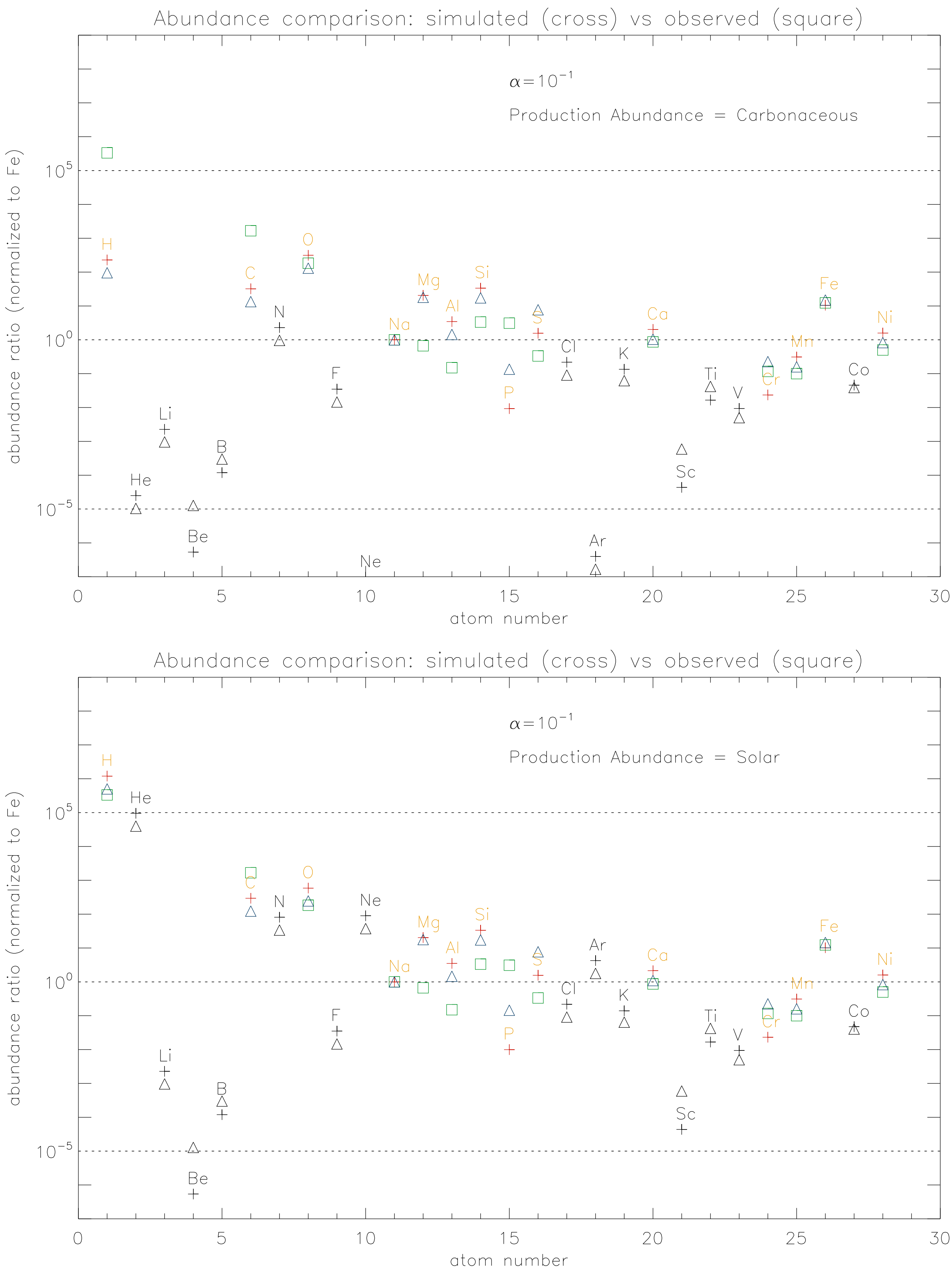


FIG. 3.— Same as figure 2 but with $\alpha = 0.1$

## APPENDIX

## A. EQUILIBRIUM VELOCITY DUE TO NEUTRAL-ION COLLISION: $V_{NEU_1}$

Being similar to Beust et al. (1989) which studied the braking of ion by in an neutral gas, here we consider a neutral atom braked by an ion gas (assumed as carbon with number density of $N_{C_{II}}$). The average net momentum loss of the neutral atom in one collision is $-m_c\mathbf{v}$, where $m_c$ is the atom mass of carbon, $\mathbf{v}$ is the neutral drift velocity relative to the field ion gas. Then the mean effect of collisions is equivalent to a force on the neutral as

$$\mathbf{F}_{neu} = -N_{C_{II}}\pi b_{ni}^2 m_c v\mathbf{v} = -k\frac{v}{v_{cl}}\,\mathbf{v}, \tag{A1}$$

Here

$$b_{ni} = \left(\frac{1}{4\pi\epsilon_0}\frac{4e^2 Pol}{\mu\, v_{cl}^2}\right)^{1/4} \tag{A2}$$

is the largest impact parameter that can lead to a physical collision between the neutral and the ion, where $\epsilon_0$ is the permittivity of free space, $e$ is the charge of an electron, $Pol$ is the polarizability of the neutral, $\mu = m_x m_c/(m_x + m_c)$ is the reduced mass, $v_{cl}$ is the neutral-ion collision velocity, and with

$$k = \pi m_c\sqrt{\frac{4e^2 Pol}{4\pi\epsilon_0}\,\frac{N_{C_{II}}^2}{\mu}}. \tag{A3}$$

The collision velocity have two parts of contribution,

$$v_{cl} \sim v_s + v, \tag{A4}$$

where $v_s$ is the sound speed of carbon ion gas. On the other hand, the neutral is subject to the gravity from the central star, which is

$$\mathbf{F}_{rad} \sim \beta\frac{GM_{star}m_x}{r^2} \tag{A5}$$

Equating $\mathbf{F}_{neu}$ to $\mathbf{F}_{rad}$ we can solve an equilibrium velocity as

$$v_{\rm neu\_1} = \frac{F_{rad} + \sqrt{F_{rad}^2 + 4k\,v_s F_{rad}}}{2k}. \tag{A6}$$

This is a the limiting drift velocity of a neutral atom due to the two competing processes, i.e., the radiation forced drift and the neutral-ion collisions. If $v >> v_s$ (and we find such assumption hold here for all the considered elements), then equation A4 is reduced to $v_{cl} \sim v$, leading to

$$\begin{aligned} v_{\rm neu\_1} &= F_{rad}/k \qquad \text{if} \qquad v >> v_s, \\ &= \frac{\beta}{\pi}\left(\frac{m_x}{m_c}\right)\left(\frac{GM_{star}}{r^2}\right)\left(\frac{4e^2 Pol}{4\pi\epsilon_0}\,\frac{N_{C_{II}}^2}{\mu}\right)^{-1/2}, \\ &\sim 0.8\beta\left(\frac{m_x}{m_c}\right)\left(\frac{m_x m_c}{m_p(m_x+m_c)}\right)^{1/2}\left(\frac{N_{C_{II}}}{100\,\mathrm{cm}^{-3}}\right)^{-1}\left(\frac{r}{100\,\mathrm{AU}}\right)^{-2}\left(\frac{M_{star}}{\mathrm{M}_\odot}\right)\left(\frac{Pol}{10\,\text{Å}^3}\right)^{-1/2}\ \mathrm{ms}^{-1}, \end{aligned} \tag{A7}$$

which is the case as considered by Beust et al. (1989).

## B. EQUILIBRIUM VELOCITY DUE TO ION-ION COLLISION: $V_{ION}$

Here we study the case where a tracer ion moving in a carbon ion gas. Following Beust et al. (1989), according to the classical theory of Coulomb scattering (or referred to as "'collision"), the average net momentum loss of the tracer ion in one collision with another carbon ion is

$$\delta p = -m_c\mathbf{v}(cos\chi - 1), \tag{B1}$$

with $\chi$ is the deflection angle given by

$$tan\frac{\chi}{2} = \frac{1}{4\pi\epsilon_0}\frac{e^2}{\mu}\frac{1}{bv_{cl}^2}, \tag{B2}$$

where $b$ is the impact parameter. $v_{cl}$ is the ion-ion collision (or impact) velocity as written in equation A4. In Beust et al. (1989), they implicitly ignored $v_s$ and took $v_{cl} \sim v$. However, in the case we consider here, the tracer ion would be efficiently braked by the carbon ions, thus we expect $v \ll v_s$ and thus $v_{cl} \sim v_s$.

The equivalent force due to ion-ion collision can be expressed as

$$\begin{aligned}
\mathbf{F}_{ion} &= vN_{c_{II}} \int_0^{b_{max}} (\delta p) 2\pi b \; \mathrm{d}b \\
&= 2N_{C_{II}} \pi b_{ii}^2 \ln\left(\frac{\mu^2}{m_c^2}\frac{\lambda_D^2}{b_{ii}^2}+1\right)\frac{m_c^2}{\mu^2} m_c v\,\mathbf{v}, \qquad \text{if} \quad v_{cl}=v_s \\
&\sim 4N_{C_{II}} \pi b_{ii}^2 \ln\left(\frac{\lambda_D}{b_{ii}}\right)\left(1+\frac{m_c}{m_x}\right) m_c v\,\mathbf{v},
\end{aligned} \tag{B3}$$

Here $b_{max}$ is the maximum acceptable value of the impact parameter, which can be taken as the Debye length $\lambda_D$

$$\lambda_D \sim \sqrt{\frac{\epsilon_0 k_B T_e}{e^2 n_e}} \sim \sqrt{\frac{\epsilon_0 k_B T_{disk}}{e^2 N_{C_{II}}}}, \quad \text{if} \quad n_e \sim N_{C_{II}} \quad \text{and} \quad T_e \sim T_{disk}, \tag{B4}$$

where $k_B$ is the Boltzmann constant, $T_e$ and $T_{disk}$ are the temperatures of the electrons and the disk, respectively, $n_e$ is the number density of electron. If we assume carbon is the major donator of electron, then we expect $n_e \sim N_{C_{II}}$. $b_{ii}$ is a characteristic impact parameter for the field ion-ion collision (solve equation B2 by taking $\chi = 90°$ and substituting $\mu$ with $m_c$),

$$b_{ii} = \frac{1}{4\pi\epsilon_0}\frac{e^2}{m_c}\frac{1}{v_s^2} \sim \frac{1}{4\pi\epsilon_0}\frac{e^2}{k_B T_{disk}} \tag{B5}$$

Thus

$$\frac{\lambda_D}{b_{ii}} = 4\pi\,\epsilon^{3/2}\,e^{-3}\,k_B^{3/2}\,T_{disk}^{3/2}\,N_{C_{II}}^{-1/2} \tag{B6}$$

Equating $\mathbf{F}_{ion}$ to $\mathbf{F}_{rad}$ we can solve an equilibrium velocity as

$$\begin{aligned}
v_{\rm ion} &= \left[\left(\frac{\beta}{4\ln(\lambda_D/b_{ii})}\right)\left(\frac{1}{\pi b_{ii}^2 r N_{C_{II}}}\right)\left(\frac{m_x^2}{m_c(m_c+m_x)}\right)\right]^{1/2}\left(\frac{GM_{star}}{r}\right)^{1/2} \\
&\sim 3.7\times 10^{-2}\beta\left[\frac{m_x^2}{m_c(m_c+m_x)}\right]^{1/2}\left(\frac{N_{C_{II}}}{100\,\mathrm{cm}^{-3}}\right)^{-1/2}\left(\frac{r}{100\,\mathrm{AU}}\right)^{-1}\left(\frac{M_{star}}{\mathrm{M}_\odot}\right)^{1/2}\left(\frac{T_{disk}}{100\,\mathrm{K}}\right)\ \mathrm{ms}^{-1}
\end{aligned} \tag{B7}$$

## C. COMPUTING THE NEUTRAL FRACTION: $F_X$

If we assume that the various gas elements have reached their ionization equilibrium, namely

$$\begin{aligned}
\Gamma_c N_{c_I} &= \eta_c N_e N_{c_{II}} \\
\Gamma_x N_{x_I} &= \eta_x N_e N_{x_{II}},
\end{aligned} \tag{C1}$$

where $\Gamma_c = \Gamma_{\mathrm{AU}_c}(r/AU)^{-2}$, $\Gamma_x = \Gamma_{\mathrm{AU}_x}(r/AU)^{-2}$ are the ionization rates of neutral C and X, and $\eta_c$ and $\eta_x$ are their recombination coefficients respectively (see table-2 for the ionization rates and recombination coefficients of various species).

In the simple case we consider here, Carbon is the field gas and it is the dominant donor of electron, namely, $N_e \sim N_{c_{II}}$. Taking this approximation to equation (C1), then we can obtain the neutral fraction of the tracer gas element, $f_x$, as the following.

$$f_x = (1+\frac{\Gamma_x}{\eta_x N_{c_{II}}})^{-1} \tag{C2}$$

where $N_{c_{II}}$ is the number density of ionized carbon (ionization state = 1) and it can be solved as

$$N_{c_{II}} = \frac{-\Gamma_c + \sqrt{\Gamma_c^2 + 4\eta_c\Gamma_c}}{2\eta_c} \tag{C3}$$

TABLE 1
Abundance of various elements.

| atomic number | atomic name | atomic masses (gram) | solar abundance (number per gram of gas) | abundance for carbonaceous chondrites (number per gram of gas) |
|---|---|---|---|---|
| 1 | H | 1.673723600032740e-24 | 4.483437633821267e+23 | 1.258128484166779e+22 |
| 2 | He | 6.646476406272443e-24 | 3.556901978565554e+22 | 1.382156428586276e+15 |
| 3 | Li | 1.152580065066100e-23 | 8.623310871985634e+14 | 1.269341342610608e+17 |
| 4 | Be | 1.496507897413562e-23 | 1.146354684875105e+13 | 1.687420778873377e+15 |
| 5 | B | 1.795208627493100e-23 | 2.692549924333715e+14 | 3.963402209124883e+16 |
| 6 | C | 1.994423481845470e-23 | 1.100494279119998e+20 | 1.767512624900727e+21 |
| 7 | N | 2.325867050477070e-23 | 3.031450549913825e+19 | 1.266595336461099e+20 |
| 8 | O | 2.656762641264740e-23 | 2.196635706168325e+20 | 1.728153203424430e+22 |
| 9 | F | 3.154758795045095e-23 | 1.307565670529496e+16 | 1.924721476960127e+18 |
| 10 | Ne | 3.350917726410370e-23 | 3.339259374981998e+19 | 5.389037068411721e+12 |
| 11 | Na | 3.817540667425015e-23 | 8.940447237207388e+17 | 1.315108111769094e+20 |
| 12 | Mg | 4.035939847490500e-23 | 1.585681826108770e+19 | 2.379871996241270e+21 |
| 13 | Al | 4.480389499376385e-23 | 1.307410211526937e+18 | 1.901151590843506e+20 |
| 14 | Si | 4.663706586574550e-23 | 1.554590025596833e+19 | 2.288338457924298e+21 |
| 15 | P | 5.143313733079080e-23 | 1.301658228432228e+17 | 1.792455514092102e+19 |
| 16 | S | 5.324518050186500e-23 | 6.916371023880311e+18 | 1.018081779930520e+21 |
| 17 | Cl | 5.887108636621301e-23 | 8.141387964050616e+16 | 1.198402850414955e+19 |
| 18 | Ar | 6.633520881610800e-23 | 1.593454776236754e+18 | 2.201839264214759e+13 |
| 19 | K | 6.492424889493430e-23 | 5.739546374503508e+16 | 8.196828356284834e+18 |
| 20 | Ca | 6.655107887583800e-23 | 9.773707490927290e+17 | 1.365680391689221e+20 |
| 21 | Sc | 7.465104160505094e-23 | 5.316697887541170e+14 | 7.826117526101099e+16 |
| 22 | Ti | 7.948501653150700e-23 | 3.765217041995530e+16 | 5.542355745092649e+18 |
| 23 | V | 8.459034344412149e-23 | 4.483437633821266e+15 | 6.599568112653674e+17 |
| 24 | Cr | 8.634154779020810e-23 | 1.999202772917527e+17 | 3.004588395254603e+19 |
| 25 | Mn | 9.122676196614945e-23 | 1.425248135467177e+17 | 2.097948698224996e+19 |
| 26 | Fe | 9.273279604324500e-23 | 1.302746441450146e+19 | 1.975293756880254e+21 |
| 27 | Co | 9.786086403638259e-23 | 3.611312629461443e+16 | 5.139608176497972e+18 |
| 28 | Ni | 9.746267510582140e-23 | 7.430940322352863e+17 | 1.093825782887814e+20 |
| 29 | Cu | 1.055206062738660e-22 | 8.192689434895311e+15 | 1.205954367326105e+18 |
| 30 | Zn | 1.085660346549800e-22 | 1.905927371381718e+16 | 2.860423072405372e+18 |

TABLE 2
Ionization rates of various elements.

| atomic number | atomic name | ionisation state | ionisation rate at 1AU $\Gamma_{\rm AU}$ $(s^{-1}atom^{-1})$ | recombination coefficient at 100k $\eta$ $(s^{-1}cm^3)$ |
|---|---|---|---|---|
| 1 | H | 0 | 0.000e+000 | 3.121e-017 |
| 3 | Li | 0 | 8.581e-002 | 1.467e-010 |
| 4 | Be | 0 | 1.612e-005 | 2.741e-011 |
| 5 | B | 0 | 1.049e-003 | 3.431e-010 |
| 6 | C | 0 | 7.912e-006 | 5.667e-011 |
| 11 | Na | 0 | 1.134e-003 | 9.620e-012 |
| 12 | Mg | 0 | 7.985e-004 | 1.628e-011 |
| 13 | Al | 0 | 1.114e+000 | 9.792e-010 |
| 14 | Si | 0 | 5.516e-003 | 9.726e-010 |
| 15 | P | 0 | 3.932e-005 | 1.828e-010 |
| 16 | S | 0 | 4.435e-005 | 2.986e-010 |
| 17 | Cl | 0 | 1.696e-006 | 2.377e-011 |
| 19 | K | 0 | 4.418e-003 | 1.129e-011 |
| 20 | Ca | 0 | 1.270e-001 | 1.078e-010 |
| 20 | Ca | 1 | 1.851e-007 | 8.172e-013 |
| 21 | Sc | 0 | 8.545e-004 | 1.521e-010 |
| 21 | Sc | 1 | 2.768e-009 | 4.914e-014 |
| 22 | Ti | 0 | 1.573e-003 | 1.585e-010 |
| 23 | V | 0 | 4.019e-003 | 5.088e-011 |
| 24 | Cr | 0 | 1.113e-003 | 4.269e-010 |
| 25 | Mn | 0 | 8.947e-004 | 4.734e-012 |
| 26 | Fe | 0 | 8.597e-004 | 8.630e-011 |
| 27 | Co | 0 | 2.799e-004 | 8.941e-012 |
| 28 | Ni | 0 | 1.243e-003 | 1.796e-011 |
| 29 | Cu | 0 | 2.787e-004 | 1.282e-010 |
| 30 | Zn | 0 | 7.225e-006 | 6.763e-012 |

Note. — In reality, the recombination coefficient varies a little bit with the temperature. But for the sake of simplicity here, we ignore such a temperature dependence and just use a constant $\eta$ value (corresponding to $\eta$ at 100 k).